The University of Nottingham

UNITED KINGDOM · CHINA · MALAYSIA

ANALYTICAL DESIGN COURSEWORK 1: "ELECTROMAGNETIC SIZING OF AN ELECTRICAL MACHINE USING MATLAB"

Pawan Kumar Dhakal [20316641]
eexpd6@nottingham.ac.uk

Contents

1. Introduction

Over the decade, the rise of PMSM has been rapidly high because of their high-power density, high torque density, high temperature, because of their ability to work under corrosive environment etc. Permanent magnet machines have wide range of applications such as aerospace, home appliances, automotive etc. In modern more-electric aircraft concept, aircraft actuation system is using permanent magnet machine as they are best match for the job. One of such kind of machines are Surface Mounted Permanent Magnet Motors (SPM). Design of electrical machine from scratch is always challenging. One of the best design approaches is to carry out some preliminary design using analytical equations and finally analyzing using Finite Element Method (FEM) with software like FEMM. We can often use iterative algorithms in preliminary design as they are lengthy and time consuming. Based on already available data or utilizing similar work experience, the analytical design is prepared with analytical equations and then this will be fine-tuned using various analytical software in detail before validation [1-5] . In this coursework similar approach is adopted.

With evolution of sustainable solutions like electric vehicles in the automotive field, the efficient design of traction motors which can power the wheels with high efficiency, high power density, high torque, which is cost effective, and has wider operating range is in demand. Although induction machines are already proving of being lower cost, used in various applications, easy to construct and reliable, permanent magnet motors are becoming popular because of their various advantages as already mentioned above. They are superior to induction motor in terms of torque, power density, power factor etc. As electric vehicles operate over wider torque-speed ranger with variable driving condition, the permanent magnet machine needs to be designed to have a total energy saving over a driving period. The EV's weight and the cost are basically related to the driving range and the battery capacity. There is a tradeoff between the energy efficiency and the static efficiency at rated power over a driving period [6].

Brushless PM drive systems are potentially evolving in the field of automotive both in hybrid and electric vehicle applications. Major advantages of brushless permanent magnet motor are high peak to continuous torque and power and they are best suitable for urban electric vehicle application. A design methodology is described in [7] for a linear electromagnetic model to determine main geometric dimensions, terminal parameters, inductance, and resistance. It also verifies the thermal performance of the lumped parameter model and the design methodology is validated using finite element analysis (FEM). Although, high speed motor seems to be a better solution, if we consider the parameters like gear ratio technology and the efficiency, high torque motor is the better choice.

The effect of Airgap (Lg) on cogging torque and noise that occurs in the brushless dc motor because of this, is described in [8]. The driving frequencies of the cogging torque are majorly dependent on the pole number and the slot numbers. In small motors, ring type permanent magnets are used whereas in big motors, segmented permanent magnets are used. The tangential reluctance due to circumferential airgap between the permanent magnet segments, generates the harmonics to the cogging torque. If we use rubber magnets between the airgaps, the reluctance variation between the airgap can be reduced [8].

Also, working condition of the motor is very important as it determines the overall performance of the motor. An optimization procedure of Permanent Magnet Assisted Synchronous Reluctance Motor (PMASR) with highway and city driving schedule, is explained in [9] for traction motor application.

2. Aim

The main objective of this course work is to design a traction motor for Electric Vehicle Application which can deliver a rated power of 150kW at base speed of 9500RPM and has maximum speed of 12000 RPM. The idea is to design a Permanent Magnet Synchronous Machine (PMSM) in terms of Surface Mounted Permanent Motor (SMPM) which can deliver the required specifications.

3. Motor Specifications

Based on the requirements, we will be designing a SPM motor which has Samarium Cobalt ($SmCo$) as permanent magnet as it has better torque and power density and is best suitable for high-speed application like electric vehicles.

The following data are considered based on some literature studies and assumptions made in such a way to meet the requirements.

Maximum phase voltage$(V) = 400/sqrt(3) = 230.94V\ (RMS)$

Number of Phase $(m) = 3$

Based on the base speed, let us calculate the rated mechanical speed

$$(w) = Base\ Speed\ x \times 2\pi/60 \quad rads - 1 = 994.84\ rads - 1$$

Rated Torque $(T) = Rated\ Power/w = 150.78\ Nm$

Generally, the power electronics (IGBT) we choose for motor drive has switching frequency of 15kHz-20kHZ.

So, our operating frequency must be at least 10 times less than the switching frequency.

So, $frequency(f) = speed * no.of\ pole\ pairs/60$

To satisfy the above equation, let us choose number of pole pairs $(p) = 4$

Total number of slots per pole per phase $(q) = total\ slots/(2 * p * m) = 3$

Which gives, total no of slots $(z) = 72$

Let us choose the length of airgap $(Lg) = 1.2e - 3\ m$

Magnet Span to Pole Span ratio $(Ka) = 83\% = 0.83$

Fundamental Peak of the Airgap Flux Density $(Bmag) = 0.8\ T$

Remanent Flux Density $(Br) = 1.04\ T$

Relative Permeability of the Magnet (μm) $= 1.02$

Slot Fill Factor ($Kfill$) = $Area\ of\ Copper/Area\ of\ Slot = 0.45$

Copper Resistivity $(\varrho cu) = 2.7e - 8\ Ohmm - 1$

Saturation Flux Density of the Yoke $(Bbi) = 1.7\ T$

Saturation Flux Density of Tooth $(Bt) = 1.68\,T$

Desired Power Factor $(pf) = 0.88$

Current Density in Copper $(J) = 11.5e6\ Am-2$

Electrical Loading $(H/A) = 42.0e3\ Am-1$

Active Axial Length $(Lz) = 0.15\,m$

4. MATLAB Scripting

To carry out the design required, a pre-built MATLAB script based on the analytical design equations is used. The following are some of the equations used.

Peak Airgap Flux Density $(Bg) = \frac{Bmag}{\frac{4}{\pi}\times sin(Ka\frac{\pi}{2})}$ Tesla

Length of Magnet $(Lm) = \frac{\mu_m \times Lg}{\frac{Br}{Bg}-1}$ $m$eters

Fundamental Winding Distribution Factor $(Kw1) = \frac{sin(\pi/6)}{q\times sin(\pi/6q)}$

Rotor Outer Diameter $(D) = \sqrt{\frac{2\times Torque}{H\times B\times Kw1\times Lz\times\pi}}$ $meters$

Peripheral Speed of Rotor $(Vmax) = (D/2)\times Max.Speed\times\frac{2\pi}{60}$ ms^{-1}

Flux per Pole $(\emptyset p) = D\times Lz\times Bmag/p$ Wb

Slot Pitch $(\tau_s) = \pi\times D/z$ m

Tooth Width $(Wt) = \tau_s\times Bmag/Bt$ $meters$

Pole Pitch $(\tau_p) = \pi\times D/2p$ m

Width of Back Iron $(Wbi) = \tau_p\times Bmag/(2\times Bbi)$ $meters$

Area of All Copper Section $(Scu-all) = \frac{\pi\times D\times H}{J\times Kfill}$ m^2

Area of Copper in One Slot $(Scu) = Scu-all/z$ m^2

Diameter of Back Iron $(Dbi) = \sqrt{\frac{8\times Scu-all}{\pi}+D^2}$ $meters$

Stator Outer Diameter $(Ds/Dext) = Dbi + 2\times Wbi$ $meters$

Length of End Windings $(Lew) = 2.5\times(D/p)$ $meters$

Total Active Length $(Ltot) = Lz + Lew$ $meters$

Copper Losses $(Pcu) = \varrho cu\times Ltot\times Scu-all\times Kfill\times J^2$ $Watts$

Back EMF $(Erms) = 2\times\pi\times fs/p\times Kw1\times Nph\times B\times Lz$ $Volts$

$where$, Number of Turns per Phase $(Nph) = H\times\pi\times D/(2\times m\times I)$,

$I\ is\ the\ rated\ phase\ current\ in\ Amps$

5. Results & Discussions

In this section, effect on motor parameters with variation of various parameters such as airgap length (Lg), permanent magnet coverage over pole (ka), airgap flux density $(Bmag)$, current density (J), electric loading (H) etc. are analyzed and discussed.

With the above-mentioned motor specifications, the following motor dimensions and parameters are obtained with the MATLAB script that was built using the analytical design equations.

Permanent Magnet Length $(Lm) = 0.0021\ m = 2.1\ mm$

Fundamental Winding Distribution Factor $(Kw) = 0.9598$

Mechanical Speed $(Wr) = 994.8377\ rads - 1$

Rotor Outer Diameter $(D) = 0.1675\ m = 167.5\ mm$

Peripheral Speed of the Rotor $(v) = 105.255\ ms - 1$

Flux Per Pole $(\emptyset_p) = 0.0050\ Wb$

Slot Pitch $(\tau_s) = 0.0073$

Pole Pitch $(\tau_p) = 0.0658$

Width of Tooth $(Wt) = 0.0035\ m = 3.5\ mm$

Width of Back Iron/ Back Iron Thickness $(Wbi) = 0.0155\ m = 15.5\ mm$

Cross-Sectional Area of One Slot $(S\_Cu) = 5.93 \times 10^{-5}\ m^2 = 59.3\ mm^2$

Diameter of Back Iron/Yoke $(Dbi) = 0.1973\ m = 197.3\ mm$ (Slot Bottom)

Stator Outer Diameter/ External Diameter $(Ds) = 0.2283\ m = 228.3\ mm$

Length of End Windings $(Lew) = 0.1047\ m = 104.7\ mm$

Total Length Including Lew $(L\_tot) = 0.2547\ m = 254.7\ mm$

Copper Losses $(Pcu) = 1.748 \times 10^3\ Watts$

RMS Phase Current $(I) = 251.769\ Amp$

Efficiency $(\eta) = 0.9772 = 97.72\%$

Number of Turns Per Phase $(Nph) = 15$

Number of Turns Per Slot $(N) = 1$

RMS Back EMF $(E) = 204\ Volts$

External Area $(Aext) = 0.1827\ m^2 = 182700\ mm^2$

5.1 Variation of Airgap Length

Airgap plays an important role in determining the quality of magnetomotive force generated by a permanent magnet machine. Figure 1 below shows how variation on airgap length changes the thickness/length of the permanent magnet. There is a direct proportion on variation of length of magnet require with the variation of airgap. Also, only the PM thickness varies with airgap. Other parameters of the machine remain unchanged.

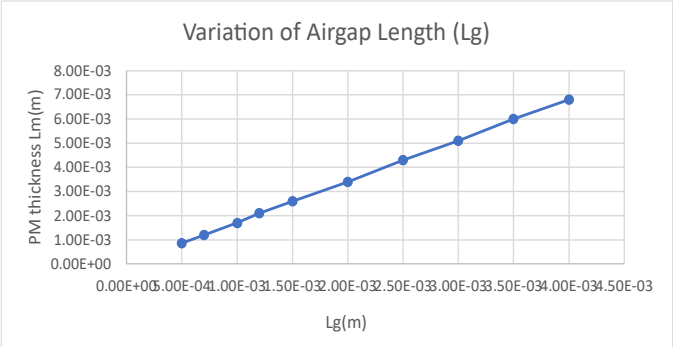

Fig. 1 Effect of variation of airgap on PM thickness

5.2 Variation of PM Coverage Over Pole

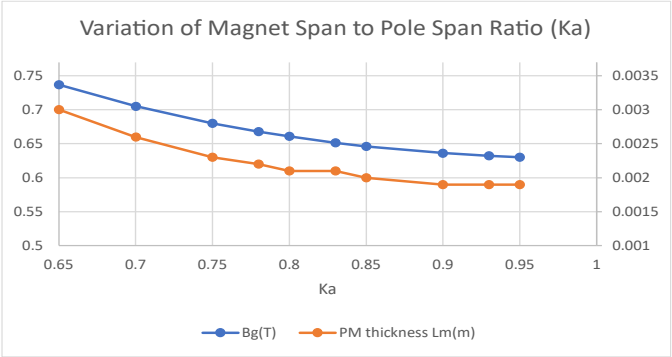

Fig. 2 Effect of Variation of Magnet Pole Span Ratio

It is clear from the figure 2 above that, when we vary the magnet span to pole span ratio (Ka) keeping the other input parameters constant, only the peak airgap flux density (Bg) and permanent magnet thickness (Lm) varies. The variation looks like a hyperbola with an increase in Ka decreases both Bg and the Lm.

5.3 Variation of Airgap Flux Density

Variation of fundamental peak of airgap flux density $(Bamg)$ is as shown in figure 3 below. Both the stator and rotor diameter decrease with increase in the $Bmag$. Variation looks somewhat hyperbolic in nature. Of course, the variations are observed keeping all other inputs constant. Copper losses (Pcu) decrease while efficiency increase with increase in $Bmag$. External area (A_ext) and the slot area (S_cu) both decrease.

Increasing $Bmag$, variations on back emf look interesting as shown below. Back emf either increases or decreases based on the proportion of increase of the flux per pole$(\emptyset p)$ and decrease of the number of turns per phase (Nph).

Both slot pitch (τ_s) and pole pitch (τ_p) decrease with increase in $Bmag$ while tooth width (Wt) and PM thickness (Lm) increase. All variations are hyperbolic in nature. In addition, length of end windings (Lew) and number of turns per phase (Nph) both decrease with increase in airgap flux density. Since peripheral

speed decreases with increase in $Bmag$, this means that my maximum speed of the motor would decrease.

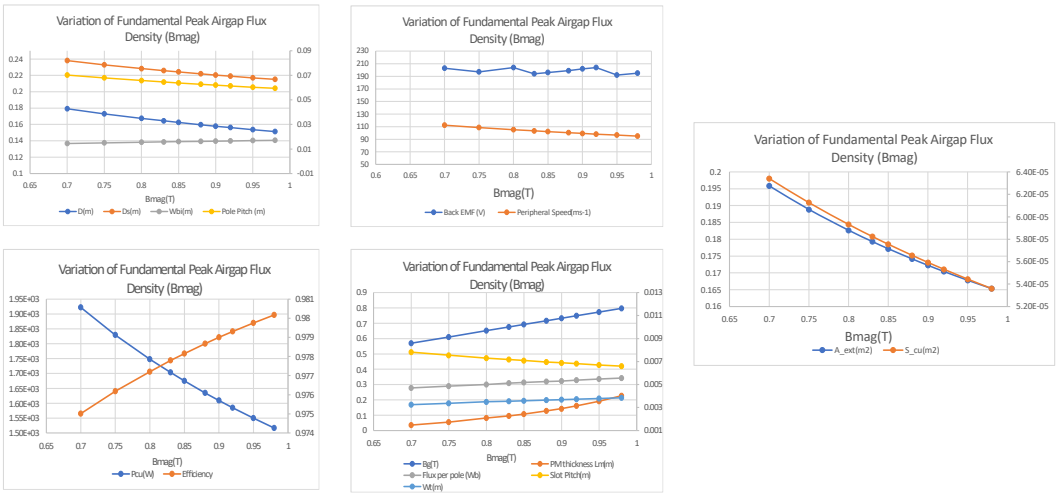

Fig. 3 Effect of Variation of Fundamental Peak Airgap Flux Density

5.4 Variation of Current Density

Variation of current density affects copper losses, outer stator diameter, efficiency, external area, and the slot area. Slot area and outer stator diameter decrease while copper losses increase and hence efficiency decreases with increase in the current density. External area shows surprising variations over the variation of J. This is mainly because, external area depends on the length of end windings (Lew) and the diameter of back iron, which eventually depends on the slot area (S_cu). So, the proportion increase or decrease depends on the proportion increase in stator outer diameter (Ds) and the proportion decrease in slot area.

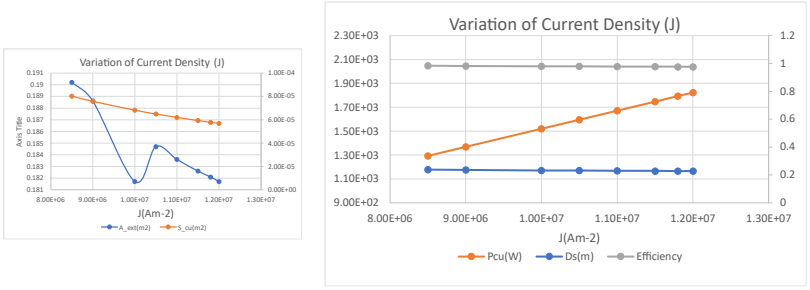

Fig. 4 Effect of Variation of Current Density

5.5 Variation of Electric Loading

Variations of electric loading (H) affects most of the motor dimensions as shown in figure 5 below. Outer rotor diameter, outer stator diameter, width of back iron, pole pitch, slot pitch, tooth width and flux per pole all decrease with increase in current loading. Like the effect of airgap flux density, the current loading variation also affects the back emf. It increases and decreases on the proportion according to the decrease of flux per pole and increase of number of turns per phase when we increase the current loading. Area of slot is directly proportional to the current loading. Moreover, length of end windings increases with decrease in current loading. Also, peripheral speed decrease with increase in current loading while copper losses increase and hence efficiency decrease. Since peripheral speed decreases with increase in my current loading, my maximum speed of the motor would decrease.

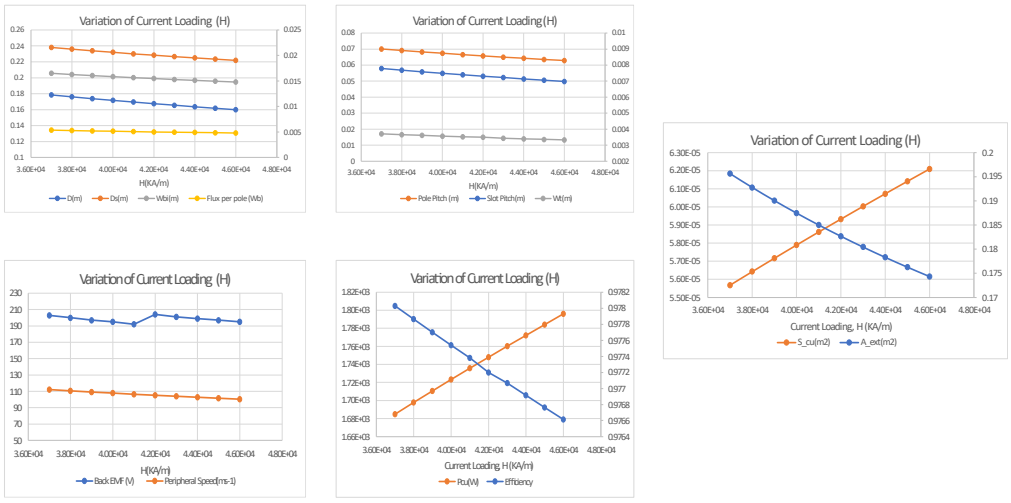

Fig. 5 Effect of Variation of Current Loading

6. Conclusion

In this coursework, a surface mounted permanent magnet synchronous motor (SMPM) with 150kW of power rating and a base speed of 9500 RMP is taken, and its specifications are studied and finally its various dimensions are analyzed with a prebuilt MATLAB script using analytical equations. The maximum speed of the motor is 12000 RPM, which will basically define the peripheral speed of the rotor. So, accordingly the mounting of permanent magnet should be done. Also, effect of variations of different input parameters on the various motor dimensions are studied and plotted. Parameters like airgap, current density, current loading, airgap flux density, and magnet pole span play an important role in determining the size of a particular motor and determine its performance. It has been clear that the variations on these parameters affects most of the motor dimensions and its performance critically. As a part of motor design process, with those dimensions, further work of analyzing it with finite element method will be carried in next coursework.

7. References

[1] S. Vaschetto, A. Tenconi, and G. Bramerdorfer, "Sizing procedure of surface mounted PM machines for fast analytical evaluations," in *2017 IEEE International Electric Machines and Drives Conference (IEMDC)*, 21-24 May 2017 2017, pp. 1-8, doi: 10.1109/IEMDC.2017.8002223.

[2] F. Marignetti, M. A. Darmani, and S. M. Mirimani, "Electromagnetic sizing of axial-field flux switching permanent magnet machine," in *IECON 2016 - 42nd Annual Conference of the IEEE Industrial Electronics Society*, 23-26 Oct. 2016 2016, pp. 1624-1628, doi: 10.1109/IECON.2016.7793175.

[3] S. Vaschetto, G. Bramerdorfer, A. Cavagnino, and A. Tenconi, "Analytically-Based Optimization of SMPM Machines for Sizing Validation Purposes," in *2019 IEEE International Electric Machines & Drives Conference (IEMDC)*, 12-15 May 2019 2019, pp. 1433-1438, doi: 10.1109/IEMDC.2019.8785195.

[4] L. Xu, Y. Xu, J. Xu, B. Wang, and F. Xin, "Optimal design and electromagnetic analysis of yokeless and segmented armature machine based on finite-element method and genetic algorithm," in *2017 IEEE Transportation Electrification Conference and Expo, Asia-Pacific (ITEC Asia-Pacific)*, 7-10 Aug. 2017 2017, pp. 1-6, doi: 10.1109/ITEC-AP.2017.8080983.

[5] S. Hlioui, L. Vido, Y. Amara, M. Gabsi, A. Miraoui, and M. Lecrivain, "Design of a synchronous machine with concentric stator windings and permanent magnets in focusing configuration," in *2007 International Aegean Conference on Electrical Machines and Power Electronics*, 10-12 Sept. 2007 2007, pp. 507-512, doi: 10.1109/ACEMP.2007.4510554.

[6] P. Lazari, J. Wang, and L. Chen, "A Computationally Efficient Design Technique for Electric-Vehicle Traction Machines," *IEEE Transactions on Industry Applications,* vol. 50, no. 5, pp. 3203-3213, 2014, doi: 10.1109/TIA.2014.2304619.

[7] N. Schofield and C. Giraud-Audine, "Design procedure for brushless PM traction machines for electric vehicle applications," in *IEEE International Conference on Electric Machines and Drives, 2005.*, 15-15 May 2005 2005, pp. 1788-1792, doi: 10.1109/IEMDC.2005.195962.

[8] J. Song, S. Sung, and G. Jang, "Effect of air gap between PM segments on cogging torque and acoustic noise of BLDC motor," in *2015 IEEE International Magnetics Conference (INTERMAG)*, 11-15 May 2015 2015, pp. 1-1, doi: 10.1109/INTMAG.2015.7157401.

[9] M. Degano, E. Carraro, and N. Bianchi, "Selection Criteria and Robust Optimization of a Traction PM-Assisted Synchronous Reluctance Motor," *IEEE Transactions on Industry Applications,* vol. 51, no. 6, pp. 4383-4391, 2015, doi: 10.1109/TIA.2015.2443091.

Appendix

Table 1 Variation of Ka

Ka	Bg(T)	PM thickness Lm(m)
0.65	0.7369	0.003
0.7	0.7052	0.0026
0.75	0.6801	0.0023
0.78	0.6678	0.0022
0.8	0.6607	0.0021
0.83	0.6514	0.0021
0.85	0.6462	0.002
0.9	0.6362	0.0019
0.93	0.6321	0.0019
0.95	0.6303	0.0019

Table 2 Variation of Current Density J

J(A/m2)	Ds(m)	Pcu(W)	Efficiency	A_ext(m2)	S_cu(m2)
8.50E+06	0.23778628	1.29E+03	0.983065	0.1902	8.03E-05
9.00E+06	0.235800418	1.37E+03	0.982086	0.1886	7.58E-05
1.00E+07	0.232379522	1.52E+03	0.980136	0.1817	6.82E-05
1.05E+07	0.230895507	1.60E+03	0.979163	0.1847	6.50E-05
1.10E+07	0.229536779	1.67E+03	0.978192	0.1836	6.20E-05
1.15E+07	0.2283	1.75E+03	0.9772	0.1826	5.93E-05
1.18E+07	0.227586121	1.79E+03	0.976643	0.1821	5.78E-05
1.20E+07	0.227136363	1.82E+03	0.976257	0.1817	5.69E-05

Table 3 Variation of Airgap

Airgap Lg(m)	PM thickness Lm(m)
5.00E-04	8.55E-04
7.00E-04	0.0012
1.00E-03	0.0017
1.20E-03	0.0021
1.50E-03	0.0026

2.00E-03	0.0034
2.50E-03	0.0043
3.00E-03	0.0051
3.50E-03	0.006
4.00E-03	0.0068

Table 4 Variation of Electrical Loading

H(KA/m)	Back EMF (V)	D(m)	Ds(m)	Wbi(m)	Peripheral Speed(ms-1)	Flux per pole (Wb)
3.70E+04	203	0.178479642	0.238077263	0.01649148	1.12E+02	0.005354389
3.80E+04	200	0.176115568	0.235923611	0.01627304	1.11E+02	0.005283467
3.90E+04	197	0.173843014	0.233874382	0.016063057	1.09E+02	0.00521529
4.00E+04	195	0.171656223	0.23192277	0.015860998	1.08E+02	0.005149687
4.10E+04	192	0.169549932	0.230062552	0.015666377	1.07E+02	0.005086498
4.20E+04	204	0.1675	0.2283	0.0155	105.255	0.005
4.30E+04	201	0.165559962	0.22659398	0.015297705	1.04E+02	0.004966799
4.40E+04	199	0.163667786	0.224975591	0.015122868	1.03E+02	0.004910034
4.50E+04	197	0.161839039	0.223428435	0.014953892	1.02E+02	0.004855171
4.60E+04	195	0.160070253	0.221948425	0.014790457	1.01E+02	0.004802108

H(KA/m)	Pcu(W)	Efficiency	Slot Pitch(m)	Pole Pitch (m)	Wt(m)	A_ext(m2)	S_cu(m2)
3.70E+04	1.68E+03	0.978029387	0.007787643	0.070088791	0.003708402	0.195624005	5.57E-05
3.80E+04	1.70E+03	0.977863993	0.007684491	0.069160422	0.003659282	0.192759265	5.64E-05
3.90E+04	1.71E+03	0.977700815	0.007585332	0.068267992	0.003612063	0.190041378	5.72E-05
4.00E+04	1.72E+03	0.97753977	0.007489916	0.067409241	0.003566627	0.18745972	5.79E-05
4.10E+04	1.74E+03	0.977380778	0.007398011	0.066582102	0.003522863	0.185004665	5.86E-05
4.20E+04	1.75E+03	0.9772	0.007309409	0.0658	0.0035	0.182667479	5.93E-05
4.30E+04	1.76E+03	0.977068659	0.007223916	0.065015245	0.00343996	0.180440214	6.00E-05
4.40E+04	1.77E+03	0.976915394	0.007141354	0.064272189	0.003400645	0.178315619	6.07E-05
4.50E+04	1.78E+03	0.976763909	0.00706156	0.063554042	0.003362648	0.17628707	6.14E-05
4.60E+04	1.80E+03	0.976614145	0.006984382	0.062859441	0.003325896	0.174348501	6.21E-05

Table 5 Variation of Airgap Flux Density

Bmag(T)	Back EMF (V)	D(m)	Ds(m)	Wbi(m)	Bg(T)	PM thickness Lm(m)	Peripheral Speed(ms-1)
0.7	203	0.179085686	0.238001804	0.014479044	0.569980287	0.001484312	1.13E+02

0.75	197	0.17301321	0.232870728	0.014987234	0.610693165	0.001741152	1.09E+02
0.8	204	0.1675	0.2283	0.0155	0.6514	0.0021	105.255
0.83	194	0.164464	0.225766102	0.015766305	0.675833769	0.002271547	1.03E+02
0.85	196	0.162517612	0.224170089	0.015955129	0.69211892	0.002435181	1.02E+02
0.88	199	0.159723405	0.22189398	0.016234249	0.716546647	0.002711529	1.00E+02
0.9	202	0.1579	0.2204	0.0164	0.7328	0.0029	99.2358
0.92	204	0.156212572	0.219060707	0.0166	0.749116949	0.003152192	98.15125342
0.95	192	0.153726271	0.217073185	0.016867576	0.773544675	0.003553386	96.58906479
0.98	195	0.15135503	0.215193089	0.017131836	0.797972402	0.004035565	95.09916985

Bmag(T)	Flux per pole (Wb)	Pcu(W)	Efficiency	Slot Pitch(m)	Pole Pitch (m)	Wt(m)	A_ext(m2)	S_cu(m2)
0.7	0.004700999	1.92E+03	0.975016657	0.007814087	0.070326785	0.00325587	0.195845216	6.34E-05
0.75	0.004865997	1.83E+03	0.976185023	0.007549125	0.067942129	0.003370145	0.18884641	6.13E-05
0.8	0.005	1.75E+03	0.9772	0.0073	0.0658	0.0035	0.182667479	5.93E-05
0.83	0.005118942	1.70E+03	0.977793871	0.007176096	0.064584862	0.003545333	0.179295131	5.82E-05
0.85	0.005180249	1.68E+03	0.978154224	0.007091169	0.063820517	0.003587794	0.177170921	5.76E-05
0.88	0.005270872	1.63E+03	0.978667675	0.006969248	0.062723234	0.003650559	0.174154615	5.66E-05
0.9	0.0053	1.61E+03	0.979	0.006891377	0.062022394	0.003691809	0.172248739	5.59E-05
0.92	0.005389334	1.58E+03	0.979306326	0.006816059	0.061344533	0.003732604	0.170420811	5.53E-05
0.95	0.005476498	1.55E+03	0.979754223	0.006707574	0.060368165	0.003792973	0.167814878	5.44E-05
0.98	0.005562297	1.52E+03	0.980177997	0.006604109	0.059436981	0.003852397	0.165359492	5.36E-05

MATLAB Script Used to Determine the Motor Dimensions

```
%%%%%%%%%%%%%%%% Analytical Design of Surface-Mount PMSM %%%%%%%%%%%%%%%%%%
clear all; clc
%%%%%%%%%%%%%% H64AEM %%%%%%%%%% Advanced Electrical Machines %%%%%%%%%%%%%%
%% Preliminary design of an SPM motor with inner rotor
% Implementation of the equations derived during the lectures of Dr. Michele Degano

%%%%%%% Data given %%%%%%%%%%%%%%%%%%%%%%%%%%%%%%%%
Torque =  150.78;            % Required rated torque [Nm]
Speed =  9500 * pi/30;    % Required rated mechanical pulsation [rad/sec]
n = 9500   %  Base Speed [rpm]
max_speed = 12000  %maximum speed in [RPM]
V = 400/sqrt(3) ;         % Maximum RMS phase voltage
%%%%%%% Data chosen or Assumed %%%%%%%%%%%%%%%%%%%%%%%%%%%%%%%%
Z = 72;                  % Number of slots
m = 3 ;                  % Number of phases
p = 4;                   % Pole pairs
```

```
fs = p* Speed /(2*pi);     % Electrical frequency at rated speed
q = Z/(2*m*p)              % Number of slots per pole/phase
Airgap = 1.2e-3;           % Airgap length [m]
Ka = 0.83;                 % Magnet span to pole span ratio
Bmg1 = 0.8;                % B*sqrt(2)(Fundamental peak airgap flux density [T])
B_g  = Bmg1 /(4/pi * sin(Ka*pi/2))     % Peak airgap flux density [T]
B = Bmg1/sqrt(2)           % Fundamental RMS airgap flux density [T]
B_mag = 1.04;              % Magnets remanent flux density [T]
Kfill = 0.45;              % Slot Fill factor (area of copper/Area of slot)
Rho = 2.7e-8;              % Copper resistivity at 100C
B_yoke = 1.7;              % Saturation flux densities in the stator yoke (back iron)
B_tooth = 1.68;            % Saturation flux densities in the stator tooth
PF = 0.88 ;                % Estimate of power factor
J = 11.5e6 ;               % Current density in the slot {4e6 [A/m^2] = 4 [A/mm^2]}
H = 42.0e3 ;               % Electrical loading [kA/m] also defined as A in the lectures
AR = 1;                    % Rotor Aspect Ratio AR = L/D
mu_m=1.02;                 % Magnet relative permeability (1)
%%%%%%%%%% Magnet thickness calculation %%%%%%%%%%%%%%%%%%%%%%%%%%%%%%%%%%%%
Lm = Airgap * mu_m*((B_g./B_mag) /(1 - (B_g./B_mag)))
Lm1 = Airgap * mu_m / ((B_mag/B_g)-1)          % Simpler way to express the PM lenght Lm [m]:
%%%%%%%%%% Fundamental Winding distribution factor calculation %%%%%%%%%%%%
Kw1 = sin(pi/6)/(q*sin(pi/(6*q)))
%%%%%%%%%% Stator, Rotor and slots dimensions %%%%%%%%%%%%%%%%%%%%%%%%%%%%%%
%D = ((2*Torque) / (H*B*AR*Kw1*pi))^(1/3); Lz = D*AR ;
Lz = 0.15;                 % Active axial lenght [m]
omega = 2*pi*n/60          % Mechanical pulsation [rad/s]
P = Torque * omega         % Mechanical power expressed at the shaft [W]
% Rotor Diameter determined from the Torque equation expressed in [m]
D = sqrt(((2*Torque)/(H*B*Kw1*pi*Lz)))
% Diameter (rotor diameter) calculated based on the demonstration
% presented during the lectures
D_validation = sqrt((120*P)/(H*Bmg1*Lz*n*sqrt(2)*(pi^2)*Kw1))

% % Airgap empirical equation g is the airgap expressed in [mm]
%g = 6*(D)/(sqrt(2*p)*1000)
% Preliminary definition of the stator geometry dimensions:
peripheral_Speed = (D/2)*2*pi*max_speed/60  %peripheral speed in meters per sec [ms-1]
fi_p = D*Lz*Bmg1/p              %Flux per pole in Wb
tau_s = pi * D / Z              % Slot pitch
Wt = tau_s * Bmg1 / B_tooth     % Tooth width
tau_p = pi * D /(2*p)           % Pole pitch
Wbi = tau_p * Bmg1 /(2*B_yoke)  % Back iron thickness (more conservative)
                        %(NOTE the Back Iron is
                        % depending on the pole number
                        %(in other words depending
                        % on the pole pitch))

% Wc = fi_p/(2*B_yoke*Lz)        %Alternative equation for back iron thickness
Scu_all = pi*D*H / (J*Kfill);   % Copper section all slots
S_cu = Scu_all/Z;               % Copper section one slot
Dbi = sqrt(8*Scu_all/pi + D^2)  % Diameter at the back iron (slot bottom)
Dext = Dbi + 2*Wbi              % External diameter (Normally called
                        % Outer Diameter OD or SOD Stator Outer Diameter)
```

```
% Calculation of the number of turns
Lew=2.5*(D/p);                  % End winding lenght (classical empirical equation)
L_tot= Lz + Lew;                % Active length including an estimated value
                        % of end-winding length
% LOSSES ESTIMATION
% Copper Losses
P_copper = Rho*L_tot* Scu_all*Kfill*J^2 ;   % Copper loss
Power = Torque*omega;                   % Mechanical output power
% With the strong hypothesis that Pjoule = Piron
I = (Power + 2*P_copper) / (3*V*PF);      % RMS phase current
Eff = Power / (Power + 2*P_copper);       % Efficiency
Nph = H * pi *D /(2*m*I);               % Number of turns per phase
N = Nph/(p*q);                          % Number of turns per slot
Nph=int32(Nph);  N=int32(N);            % Get integer numbers of turns
%%%%%%%% RMS Back EMF %%%%%%%%%%%%%%%%%
E1 = 2*pi*fs/p * Kw1*Nph*B*D*Lz;
%%Temerature rise%%
A_ext = pi*Dext*L_tot; %+ pi*Dext^2/4 ;     % External area
h = (2*P_copper)/(70 * A_ext) ;             % Heat convection transfer coeff
DT = (2*P_copper)/(h*A_ext);                % Temperature differential
%%%%%%%Spread sheet display %%%%%%%%%%%%%%%%%%%%%%%%
disp(['Inner stator Diameter: ',num2str(D*1e3),' mm']);
disp(['Active axial length: ',num2str(Lz*1e3),' mm']);
disp(['Total axial length (with EW): ',num2str(L_tot*1e3),' mm']);
disp(['Magnet thickness: ',num2str(Lm*1e3),' mm']);
disp(['External Diameter: ',num2str(Dext*1e3),' mm']);
disp(['Tooth width: ',num2str(Wt * 1000),' mm']);
disp(['Slot Depth: ',num2str((Dbi-D)/2 * 1000),' mm']);
disp(['Phase current: ',num2str(I),' A']);
disp(['Number of turns per phase: ',num2str(Nph),' turns']);
disp(['Number of turns per slot: ',num2str(N),' turns']);
disp(['EMF ',num2str(E1),' V']);
disp(['Efficiency ',num2str(Eff*100),' %']);
disp(['Temperature rise ',num2str(DT),' deg C']);
```